Supplement of Solid Earth, 11, 363–378, 2020
https://doi.org/10.5194/se-11-363-2020-supplement


Solid Earth Open Access EGU

*Supplement of*

# Subsidence associated with oil extraction, measured from s time series analysis of Sentinel-1 data: case study of the Patos-Marinza oil field, Albania

**Marianne Métois et al.**

*Correspondence to:* Marianne Métois (marianne.metois@univ-lyon1.fr)

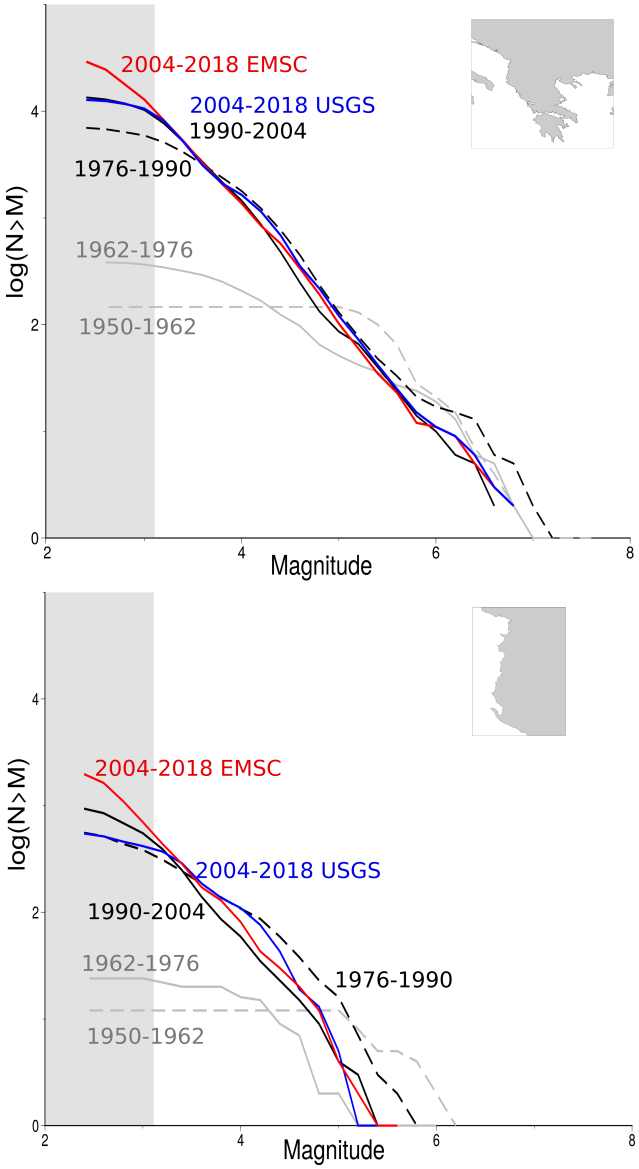


**Figure S1.** Test of the Gutemberg-Richter relationship over the southern Balkans area (top) and Albania (bottom) for different time- spans and catalogs. Map inserts in the top right corner of the graphs show the region over which the seismicity is considered. Since 1990, the completeness magnitude can be safely estimated between 3 and 3.5. Interestingly, EMSC catalog is much more complete than USGS catalog for Albania on the 2004-2018 time span.

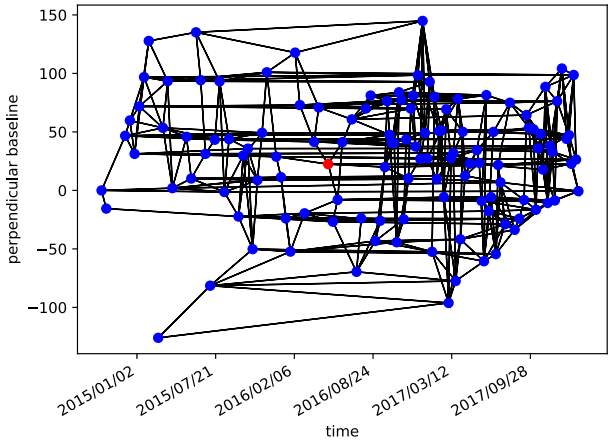


**Figure S2.** Interferometric network for descending track T153. Red circle indicates the master image.

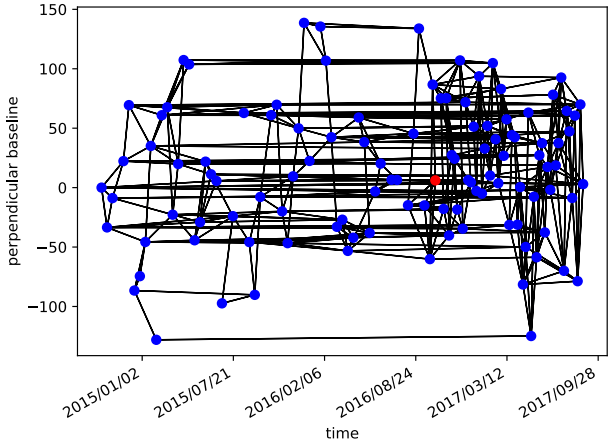


**Figure S3.** Interferometric network for ascending track T175. Red circle indicates the master image.

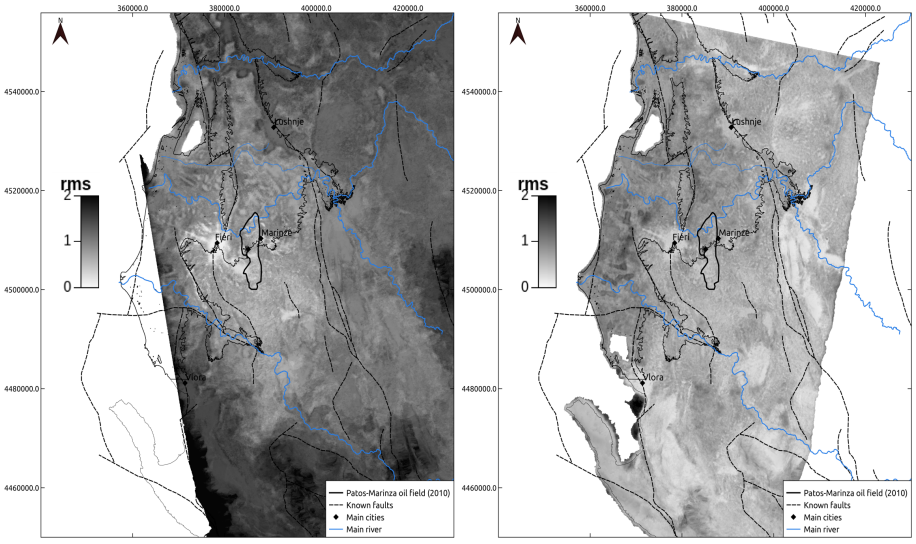


**Figure S4.** Large-scale view of the root mean square value by pixel for the ascending (left) and descending (right) tracks, given in radian. Reference areas for interferograms are chosen near Fieri (40.71°N,19.56°E) and Berat (40.73°N,19.93°E) cities, respectively.

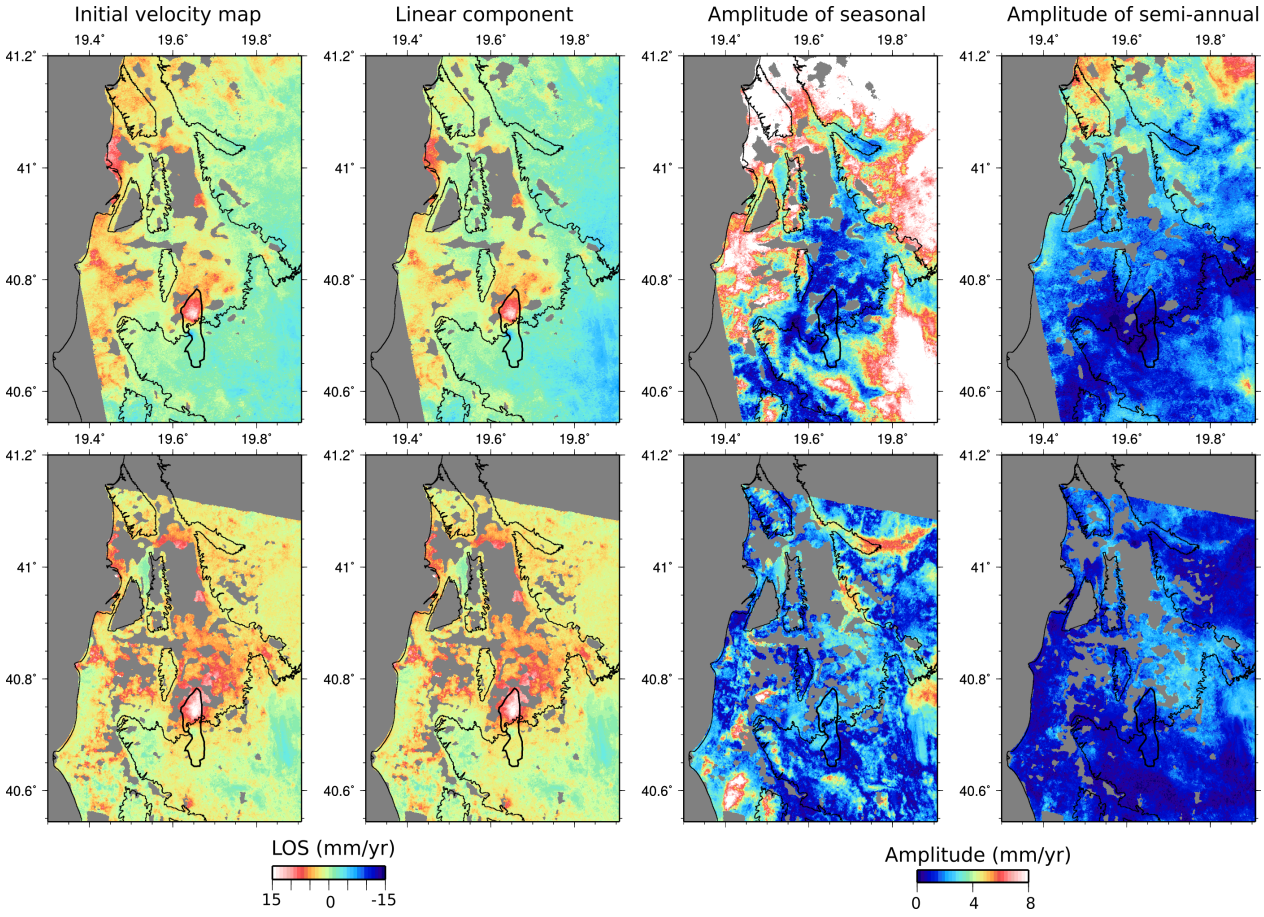


**Figure S5.** Decomposition of the estimated average velocity map (left) in linear plus annual and semiannual sinusoidal terms for ascending (top) and descending (bottom) tracks. The amplitude $\sqrt{(a^2+b^2)}$ is plotted for the annual ($T = 1$yr) and semiannual ($T = 0.5$yr) terms in mm/yr, with velocity being $a.cos(2\pi t/T) + b.cos(2\pi t/T)$.

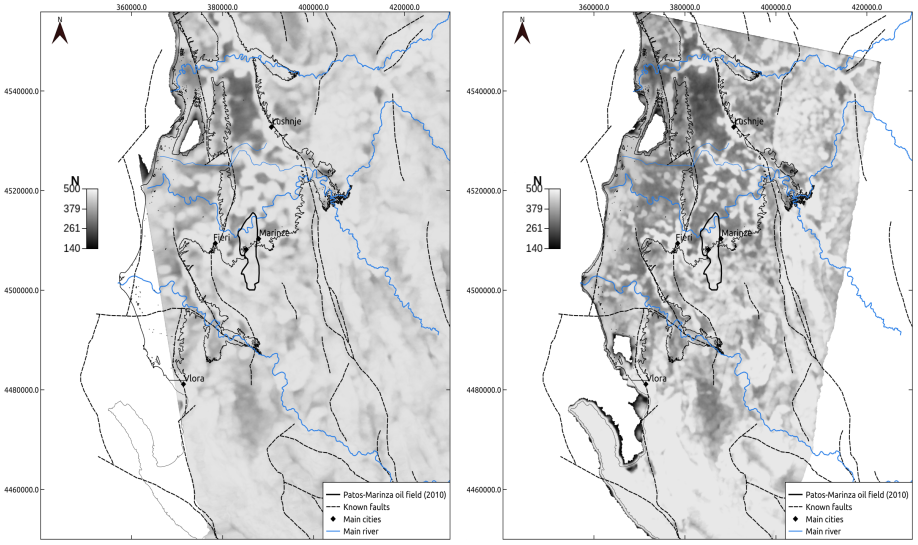


**Figure S6.** Large-scale view of the number of interferograms by pixel used in the time-series analysis to estimate the average velocity for the ascending (left) and descending (right) tracks. Based on these maps, we choose to discard pixels with less than 370 interferograms ($\sim$75% of the total interferograms) to avoid poorly constrained average velocities.

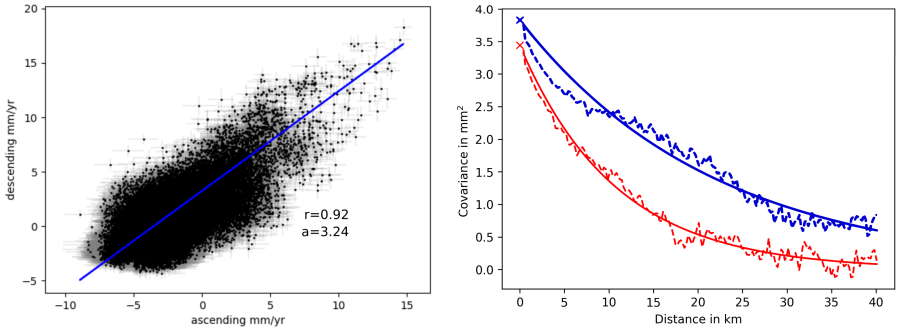


**Figure S7.** Left: Descending versus ascending LOS velocities for each pixel after masking based on Fig. S6. The very high correlation coefficient argues in favour of a consistent signal mainly due to vertical motion. The a value (given in mm/yr) is used as a constant to make both tracks consistent. Right: Covariograms of a stable portion of the ascending (red) and descending (blue) tracks (dashed curve), together with the best spherical model (plain curve). The covariance value for zero distance, equivalent to the overall variance of the image, is indicated as a red cross and differs by less than 0.5 $mm^2$ between both tracks. However, despite this similar variance, covariance is slightly higher at intermediate distances (10 to 20 km) for the descending track.

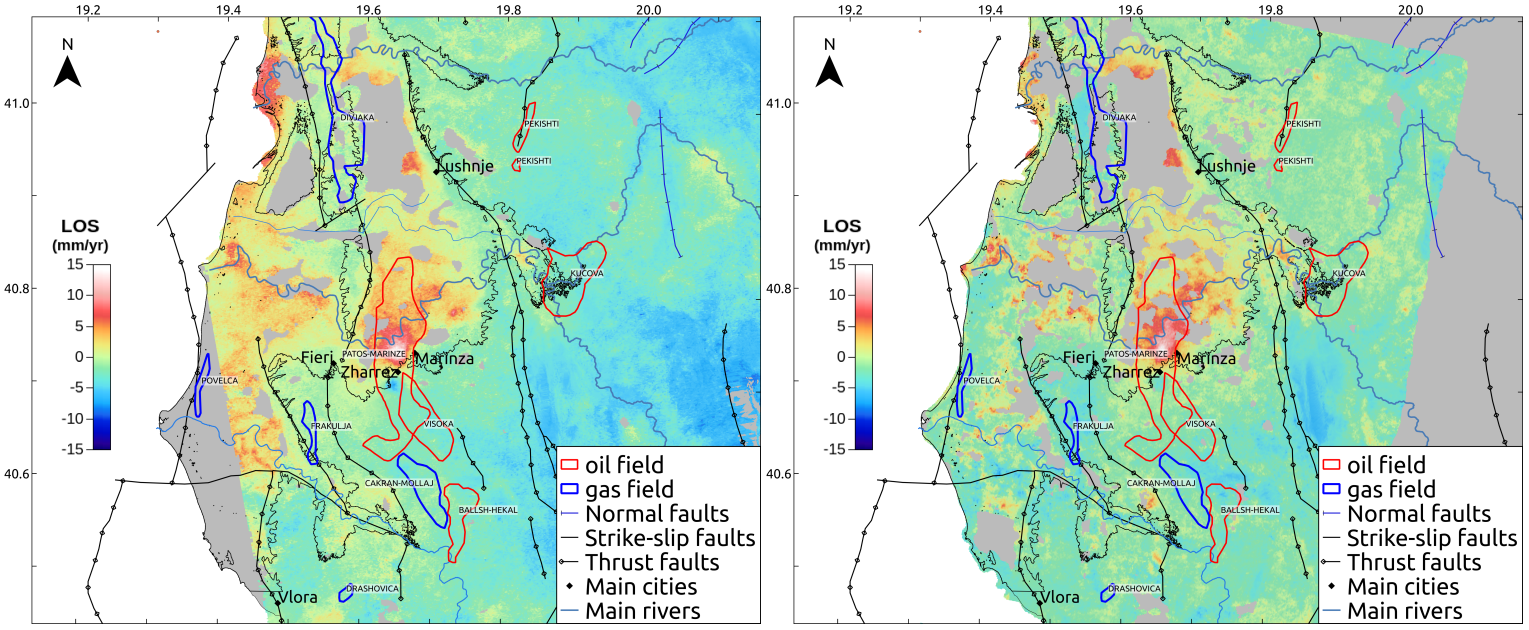


**Figure S8.** LOS velocity maps (left and right : ascending and descending tracks, respectively) together with the main known faults and the location of major oil and gas fields which name is indicated. The fields contours have been extracted from the IHS map of Albanian ressources of february 2001. The contour of the Patos-Marinza oil field is slightly different from the one plotted in Figures 1 to 6 of the main text, that has been extracted from a more recent reference (BCP, 2015). Surface deformation is only observed over the Patos-Marinza field.